

Miniaturized and Lightweight ESPAR Antenna for WSN and IoT Applications

Luiza Leszkowska*¹, Mateusz Czeleń*², Mateusz Rzymowski*³, Krzysztof Nyka*⁴, Łukasz Kulas*⁵

*Department of Microwave and Antenna Engineering, Gdansk University of Technology, Faculty of Electronics, Telecommunications and Informatics, Gdansk, Poland

{¹luiza.leszkowska, ²mateusz.czeleń, ³mateusz.rzymowski, ⁴krzysztof.nyka, ⁵lukasz.kulas}@pg.edu.pl

Abstract— A new compact ESPAR antenna is investigated in this paper. The proposed antenna has 12 directional radiation patterns based on 12 passive elements and can be successfully used in Wireless Sensor Network applications. In proposed antenna design, the possibilities of 3D printing were used to implement a dielectric miniaturization overlay that allowed for reducing antenna occupied area by almost 60% and antenna profile by 27% in comparison to the standard ESPAR antenna. The total dimensions of the antenna are 98 mm in diameter and 20.25 mm in height, while the weight of the antenna is only 86 g, which makes it much more suitable for potential use in UAV-based wireless communication applications.

Index Terms— reconfigurable antenna, antenna miniaturization, 3D printing, switched-beam antenna, electronically steerable parasitic array radiator (ESPAR) antenna, Internet of Things (IoT), wireless sensor network (WSN).

I. INTRODUCTION

In many Internet of Things (IoT) applications, Wireless Sensor Network (WSN) nodes are deployed as standalone devices (e.g. gateways) or are integrated within different objects to provide sensing, monitoring, actuating capabilities and also communication means for the whole IoT system [1]. One of the key concerns in every IoT deployment is wireless link reliability, especially when propagation conditions can change over time during a system operation. To address this challenge, beam reconfigurable antennas were proposed as, by using electronically steerable directional beams, it is possible to improve resilience of the WSN as well as scalability and energy efficiency of the whole system [2]-[4].

One of the most promising concepts of beam reconfigurable antennas that can be used in IoT or WSN systems are low-cost and energy efficient electrically steerable passive array radiator (ESPAR) antennas [5], [6] as they can provide not only network resilience, scalability and energy efficiency [7] but also 2D direction-of-arrival estimation and localization capabilities to the IoT system [5], [8]-[10]. Typical construction of low-cost and energy efficient ESPAR antenna consists of a single active element connected to a wireless transceiver output and a number of passive elements surrounding the active element and connected to variable reactances via electronically steerable FET SPDT switches. The switches can be individually controlled by I/O ports of a simple microcontroller, which is usually a part of a wireless transceiver. In consequence, one can shorten electronically a set of chosen ESPAR antenna passive

elements to the ground (while the rest is left open) directional antenna can be formed.

One of the biggest challenges connected with ESPAR antenna applications in practical IoT systems is its size. Due to the required spacing between the active and passive elements ($\sim \lambda/4$), the size of 2.4 GHz ESPAR antenna is approximately 16 cm x 3 cm, which is considerably bigger than an IoT module size. In UHF frequency band, the problem is even more pronounced as the antenna size (approximately 8.4 x 50 cm) is considerably bigger than the size of a LoRa module [11]. An obvious way to miniaturize ESPAR antenna is to embed active and passive elements in a dielectric overlay [12], which allowed the authors to miniaturize 6 element ESPAR antenna, which resulted in only 6 directional radiation patterns, using a dielectric material having $\epsilon_r=4.5$. However, the overall structure was not a low-profile due to the use of the ground plane skirt in the ESPAR antenna prototype. Currently, the similar effect at lower cost can be reached utilizing 3D print technology. The measurement results for 12 element low-cost energy efficient ESPAR antenna prototypes prepared using low-cost commonly used polylactic acid (PLA) filament and different PLA miniaturization overlays were recently reported [13]-[15]. Because, PLA dielectric constant is low and, in consequence, miniaturization using this material is limited, the original concept of 3D printed overlays was extended in simulations to be used with other filament materials available for 3D printing process [14]. However, until now, according to best authors knowledge, there are no publications available that are presenting measurement results of miniaturized ESPAR antenna prototypes produced using new 3D printed materials having high ϵ_r values that are available for radio frequency (RF) applications different than PLA. Additionally, in all available publications, the aspect of the antenna weight was not taken into account.

In this paper, we present simulation and measurement results of 12 element low-cost and energy efficient ESPAR antenna that was miniaturized using a 3D printed overlay based on PREPERM® 3D ABS400 filament having $\epsilon_r=4.0$. Comparing to the previously published results, the antenna is much more compact, then when PLA material was used. Additionally, in this paper we compare weight of ESPAR antennas miniaturized using different overlays and show, that it is possible to reach not only lower size but also lower weight when compared to the original ESPAR antenna. In result, the proposed compact ESPAR antenna can be used in IoT applications, in which the antenna size and low

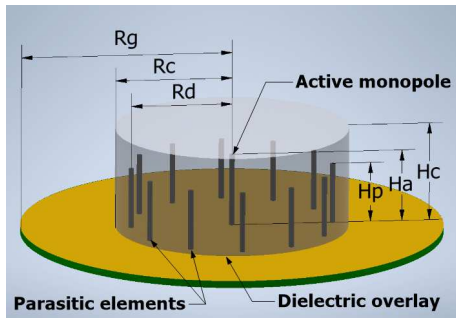


Fig. 1. Dimensions of miniaturized reconfigurable ESPAR antenna.

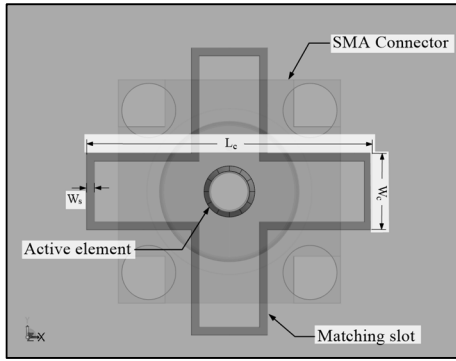


Fig. 2. Additional matching in the form of a slot between active element and ground plane

profile play an important role, including the use for UAV-based wireless communication.

II. ANTENNA DESIGN

The presented antenna design is based on the ESPAR antenna concept, which uses array of passive elements to shape antenna's beam and a dielectric overlay [13]-[15]. To make the antenna design even more compact and the whole production process more accessible and straightforward, one side of a PCB has been utilized as antenna ground plane, while the other side has been used to place steering circuit based on SPDT switches that allows to control antenna radiation pattern using GPIO pins. The integrated FET switch NJG1681 has been chosen for its very low insertion loss (0.23 dB @2.7 GHz) and very simple bias and control circuit requiring just one external inductor and capacitor [5]. All these nonidealities were taken into account in the antenna design as the realistic switch model and PCB layout of the control circuits were included in the simulations.

The antenna employs a circular ground plane, on which a single, active monopole, connected to an IoT module or a gateway, and 12 passive elements (vertical wires) are mounted. Connecting each passive element to the SPDT switch allows one to change its function between director and reflector by loading it with open or short circuit, respectively. In the proposed antenna design, opening five consecutive and shorting remaining seven passive monopoles provides a directional radiation pattern with maximum gain aligned with the third open element. The circular shift of switch states

TABLE I. COMPARISON OF THE DIMENSIONS OF PROPOSED ANTENNA WITH MINIATURIZED ESPAR ANTENNA USING PLA FILAMENT AND STANDARD NON-MINIATURIZED ESPAR ANTENNA

Parameter	Standard ESPAR antenna		Miniaturized ESPAR Antenna using PLA filament [13]		Presented miniaturized ESPAR antenna	
	Value [mm]	Value [λ_0]	Value [mm]	Value [λ_0]	Value [mm]	Value [λ_0]
R_g	76.2	0.62	59.0	0.48	49.0	0.40
R_d	45.0	0.37	28.2	0.23	20.2	0.17
H_a	24.1	0.20	20.4	0.17	19.4	0.16
H_p	28.5	0.23	16.8	0.14	14.4	0.12
R_c	-	-	32.4	0.26	23.4	0.19
H_c	-	-	24.4	0.20	20.6	0.17

TABLE II. COMPARISON OF THE DIMENSIONS REDUCTION RATIO OF PROPOSED ANTENNA AND MINIATURIZED ESPAR ANTENNA USING PLA FILAMENT COMPARED TO STANDARD ESPAR ANTENNA

Parameter		R_g	R_d	H_a	H_p	H_c
Reduction Ratio	PLA [13]	0.23	0.37	0.17	0.41	0.14 ^a
	Presented antenna	0.36	0.45	0.20	0.49	0.28 ^a

^a. Compared to the H_p of the Standard ESPAR antenna

rotates the main beam direction in the horizontal plane. All radiators have been embedded in the cylindrical shaped dielectric overlay as shown in Fig. 1. in order to reduce antenna's size. The detailed dimensions of the presented antenna and the dielectric overlay are given in the Table I. The overlay was designed for dielectric constant equal to 4.0 which corresponds to the dielectric constant of PREPERM® 3D ABS400 filament. Based on previously simulated data [14], a filament with this dielectric constant was chosen as a compromise between antenna size and gain. This allowed for reducing antenna base radius by 36% and therefore occupied area was reduced by almost 60% in comparison to the standard ESPAR antenna without dielectric overlay. Table II presents the detailed comparison of the antenna dimensions reduction ratio in reference to the miniaturized ESPAR antenna using PLA filament [13].

Introducing relatively high permittivity material comes with a design problem, which is providing a satisfactory shape of radiation pattern along with good impedance matching. The reflection coefficient is decreased to an acceptable level at a cost of degradation of far-field characteristics. Hence, to mitigate this trade-off, additional matching by means of a slot between active element and ground plane, initially introduced in [14], has been applied. Its meander layout was determined by the SMA connector PCB footprint as shown in Fig. 2. Impedance matching is achieved by modifying the total slot length L_s which in this case is equal to 9 mm. The total width of the matching slot W_c is 2.4 mm, while the width of the slot W_s is equal 0.25 mm.

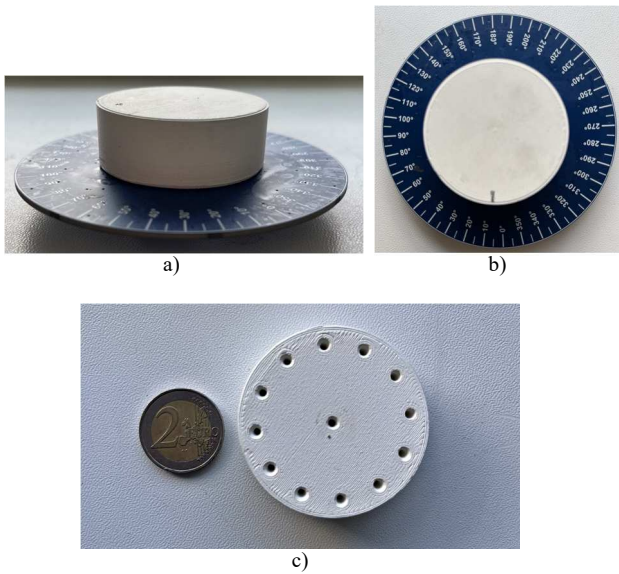


Fig. 3. Prototype of the proposed miniaturized ESPAR antenna: a) side view; b) top view; c) 3D printed dielectric overlay

TABLE III. COMPARISON OF PROPOSED ANTENNA CHARACTERISTICS WITH STANDARD NON-MINIATURIZED ESPAR ANTENNA

Parameter	HPBW E-plane [°]	Angle of maximum radiation [°]	No. of directional beams	Overall dimensions [mm]	Weight [g]
Standard ESPAR antenna	64.5	60	12	\varnothing 152.4 H 27.85	82
ESPAR antenna with PLA overlay [13]	83.7	48	12	\varnothing 118 H 26.05	144
Presented ESPAR antenna	81.5	40	12	\varnothing 98 H 20.25	86

III. REALIZATION AND MEASUREMENTS

The overlay was manufactured using FDM 3D printing technology and PREPERM® 3D ABS400 filament of dielectric constant equal to 4.0. Fig. 3. (a) and (b) shows the top and side views of the prototype of antenna respectively, while in Fig. 3 (c) bottom view of the dielectric overlay is presented. The diameter of the antenna is 98 mm and the total height is 20.25 mm. The radiation pattern of the antenna was verified in the elevation plane as shown in Fig. 4. In Fig. 5, radiation patterns for three different vertical angles are presented. Realized gain of the antenna is 3.2 dBi. The measurement results are mostly consistent with the simulation results, and only minor differences in these characteristics occurred as a result of the overlay shifts, which is discussed later in this section.

Despite significant miniaturization the antenna completely retains its reconfigurable properties allowing for 12 switched directional beams. The half power beamwidth (HPBW) of the antenna and the direction of its maximum radiation can be adjusted depending on the propagation conditions by changing the appropriate dimensions and shape of the overlay [15]. Table III shows a similarity in characteristics of the

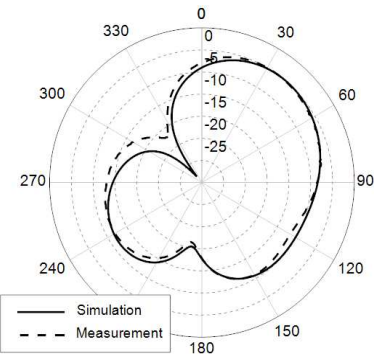


Fig. 4. Radiation pattern of the single directional beam in E-plane at 2.45 GHz

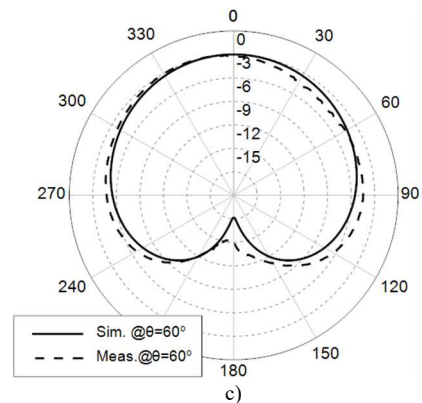
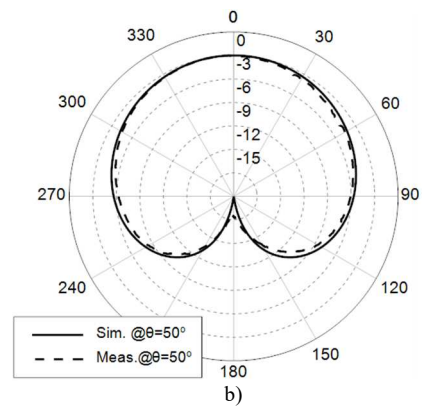
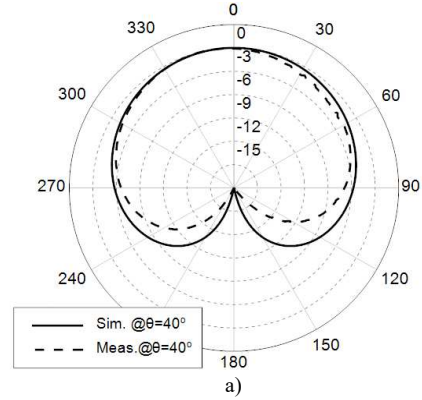


Fig. 5. Radiation pattern of the single directional beam in: a) at $\varphi = 40^\circ$; b) at $\varphi = 50^\circ$; c) at $\varphi = 60^\circ$.

TABLE IV. COMPARISON OF PROPOSED ANTENNA CHARACTERISTICS WITH STANDARD NON-MINIATURIZED ESPAR ANTENNA

Horizontal				
Overlay shift [mm]	0.1	0.2	0.3	0.365
Detuning [MHz]	8.4	26.6	62.8	98.1
Vertical				
Overlay shift [mm]	0	0.3	0.6	0.9
Reflection coefficient [dB]	-13.9	-20.9	-26.3	-34.1

proposed antenna compared to the original (non-miniaturized) version. What is of paramount importance, the new antenna achieved a significant reduction in size, when compared to the original antenna. What is equally important, the weight of the proposed antenna is almost identical to the weight of the standard ESPAR antenna despite the added dielectric overlay. The weight of miniaturized ESPAR antennas using an PLA overlay [13] was 144 g, which is significantly higher.

An important issue is the sensitivity of antenna performance towards the placement of active and passive elements in the holes of the overlay. The higher degree of miniaturization, the more significant impact the air gaps in the overlay around the active and passive elements have on the antenna's parameters. It is particularly visible in the shift of resonant frequency. The air gap inaccuracies resulting from the 3D-printing production process of the overlay and the misalignment of the overlay and the antenna wires of 0.1 mm may result in detuning the antenna frequency by 8.4 MHz, while 0.365 mm, which is the maximum possible shift of the overlay in the presented prototype, by 98.1 MHz. Also, an inaccuracy of mounting the dielectric overlay to the base antenna in the vertical axis (along the active element) affects the antenna performance. An air gap between the base antenna and the overlay, causes differences in the S11 level. This effect is shown in Table IV, for three vertical and four horizontal different random overlay placement. In consequence, in practical designs, one has to take special care of the proper dielectric overlay placement with respect to antenna elements.

IV. CONCLUSIONS

In this paper, the most compact low-cost and energy efficient ESPAR antenna ever produced is presented. Miniaturization of the antenna was carried out using a 3D printed overlay and, as a result, the dimensions of the antenna allow for its practical use in WSN application in which the antenna size and profile has to be low. In addition, the use of a filament with a higher than PLA dielectric constant to produce the overlay, made it possible to reduce the size of the antenna while keeping the total weight almost unchanged compared to the non-miniaturized antenna. This allows considering the use of this type of antenna in UAV-based wireless communication.

ACKNOWLEDGMENT

This research was funded by the i-MAGS project, which has received funding from the Federal Ministry of Education

and Research (BMBF; agreement no. 01DS22002A) and the National Centre for Research and Development (NCBR; agreement no. WPN/4/66/i-MAGS/2022) under 4th Poland – Germany Call for Proposals in the field of Digital Green Technology.

REFERENCES

- [1] Joshi, G. P., Nam, S. Y., & Kim, S. W. (2013). Cognitive Radio Wireless Sensor Networks: Applications, Challenges and Research Trends. *Sensors* 2013, 13, 11196–11228.
- [2] T. Loh, K. Liu, F. Qin, H. Liu, "Assessment of the adaptive routing performance of a wireless sensor network using smart antennas," *IET Wireless Sensor Systems*, vol. 4, no. 4, pp. 195-205, 2014
- [3] F. Viani, L. Lizzi, M. Donelli, D. Pregnotato, G. Oliveri, and A. Massa, "Exploitation of parasitic smart antennas in wireless sensor networks," *Journal of Electromagnetic Waves and Applications*, vol. 24, no. 7, pp. 993-1003, Jan. 2010.
- [4] E. D. Skiani, S. A. Mitilneos, S. C. A. Thomopoulos, "A study of the performance of wireless sensor networks operating with smart antennas," *IEEE Antennas and Propagation Magazine*, vol. 54, no. 3, pp. 50-67, 2012.
- [5] M. Groth, M. Rzymowski, K. Nyka and L. Kulas, "ESPAR Antenna-Based WSN Node With DoA Estimation Capability," in *IEEE Access*, vol. 8, pp. 91435-91447, 2020.
- [6] M. Burtowy, M. Rzymowski, and L. Kulas, "Low-Profile ESPAR Antenna for RSS-Based DoA Estimation in IoT Applications," *IEEE Access*, vol. 7, pp. 17403-17411, 2019.
- [7] F. Ademaj, M. Rzymowski, H.-P. Bernhard, K. Nyka, L. Kulas, "Relay-aided Wireless Sensor Network Discovery Algorithm for Dense Industrial IoT utilizing ESPAR Antennas". *IEEE Internet of Things Journal*, vol. 8, no. 22, pp. 16653 - 16665, 2021.
- [8] L. Kulas, "RSS-based DoA Estimation Using ESPAR Antennas and Interpolated Radiation Patterns," *IEEE Antennas Wireless Propag. Lett.*, vol. 17, no. 1, pp. 25-28, Jan. 2018.
- [9] L. Kulas, "Simple 2-D Direction-of-Arrival Estimation Using an ESPAR Antenna," in *IEEE Antennas and Wireless Propagation Letters*, vol. 16, pp. 2513-2516, 2017, doi: 10.1109/LAWP.2017.2728322.
- [10] M. Groth, K. Nyka, and L. Kulas, "Calibration-Free Single-Anchored Indoor Localization Using an ESPAR Antenna," *Sensors*, vol. 21, no. 10, p. 3431, May 2021, doi: 10.3390/s21103431.
- [11] M. Rzymowski, D. Duraj, L. Kulas, K. Nyka and P. Woznica, "UHF ESPAR antenna for simple Angle of Arrival estimation in UHF RFID applications," 2016 21st International Conference on Microwave, Radar and Wireless Communications (MIKON), Krakow, Poland, 2016, pp. 1-4.
- [12] Junwei Lu, D. Ireland and R. Schlub, "Dielectric embedded ESPAR (DEESPAR) antenna array for wireless communications," *IEEE Trans. Antennas Propag.*, vol. 53, no. 8, pp. 2437-2443, Aug. 2005.
- [13] M. Czelen, M. Rzymowski, K. Nyka and L. Kulas, "Miniaturization of ESPAR Antenna Using Low-Cost 3D Printing Process," 2020 14th European Conference on Antennas and Propagation (EuCAP), Copenhagen, Denmark, 2020, pp. 1-4.
- [14] M. Czelen, M. Rzymowski, K. Nyka and L. Kulas, "Influence of Dielectric Overlay Permittivity on Size and Performance of Miniaturized ESPAR Antenna," 2020 23rd International Microwave and Radar Conference (MIKON), Warsaw, Poland, 2020, pp. 289-292.
- [15] M. Czelen, M. Rzymowski, K. Nyka and L. Kulas, "Influence of Dielectric Overlay Dimensions on Performance of Miniaturized ESPAR Antenna," 2020 IEEE International Symposium on Antennas and Propagation and North American Radio Science Meeting, Montreal, QC, Canada, 2020, pp. 387-388.